

Proposal and analysis of digital concatenated gratings

Xiaoying He,^{1,2,*} Dexiu Huang,¹ Yonglin Yu,¹ and D. N. Wang²

¹Wuhan National Laboratory for Optoelectronics, Huazhong University of Science and Technology, Wuhan 430074, China

²Department of Electrical Engineering, The Hong Kong Polytechnic University, Hung Hom, Kowloon, Hong Kong

*Corresponding author: hxyhust@yahoo.com.cn

Received March 14, 2008; accepted April 26, 2008;
posted May 5, 2008 (Doc. ID 93894); published June 19, 2008

A digital concatenated grating composed of five subgratings is proposed. Essential formulas on Bragg periods of subgratings and an analytical expression for the reflection-spectrum envelope are presented, which show how to use reflection-spectrum envelopes to construct a digital concatenated grating with uniform reflection peaks. For a perfect design, the spectral center separation of adjacent Bragg gratings will be chosen as the integral times of the reflectivity peaks' spacing. Gaussian apodization on the whole profile grating not only eliminates the sidelobes of each reflection peak but also provides a better flat reflection-spectrum envelope than that of the digital concatenated Gaussian-apodized grating. © 2008 Optical Society of America

OCIS codes: 060.2340, 060.3735, 070.4790.

1. INTRODUCTION

Sampled gratings (SGs) are pivotal components for optical communications and optical fiber sensor systems because of their wide applications in tunable semiconductor lasers [1,2], multichannel dispersion compensation [3,4], multichannel signal processing [5,6], etc. However, the uneven reflection-spectrum envelope of sampled gratings is a key factor that limits their applications. Especially, in tunable sampled-grating distributed Bragg reflector (SG-DBR) lasers, sampled gratings with a sinc spectrum envelope have a large output power variation over the whole tuning range. Various kinds of designs and writing techniques have been proposed for obtaining a broad flat-top reflection-spectrum envelope, including multiple phase shifts [7,8], sinc-function apodization [9], the interleaved technique [10], and multiple reflection-spectrum envelopes concatenated (MRSEC) technology [11].

The interleaved technique consists of interleaving several sampled gratings to increase the strength and bandwidths of the individual channels and shorten the reflection-peak spacing [5]. That is, interleaving N sampled gratings can reduce the sampling period by $1/N$ times. However, this technology may result in the disappearance of some peaks in the specified wavelength.

Another approach is to use multiple phase shifts to obtain uniform reflection peaks over a large spectral region [7], but in this approach it is necessary to modify the relative phase of the channels, similarly to appending the phase-only sampling function in the conventional Bragg grating.

The MRSEC technology is used for concatenating a series of reflection-spectrum envelopes of sampled gratings with different Bragg wavelengths to obtain a broad flat-top reflection-spectrum envelope. By a careful selection of the Bragg wavelengths of the sampled gratings, a new

type of multipeak grating is obtained, called the digital concatenated grating.

In this paper, the schematic structure of the digital concatenated grating (DCG) is illustrated. An analytical formula for the reflection-spectrum envelope is used to demonstrate the advantage of the DCG. The impact of the parameter m on the reflection spectrum of the DCG is also discussed. A Gaussian tailoring of coupling strength along the DCG is also introduced into the sampling function and the whole grating profile function.

2. DESIGN OF DIGITAL CONCATENATED GRATINGS

A. Theoretical Formulas

An application of the MRSEC technology is shown in Fig. 1, where the DCG is composed of five ($M=5$) sampled gratings called subgratings. In Fig. 1(a), all the reflection-spectrum envelopes of the subgratings have identical shapes, and the spectral center separation $\Delta\lambda$ between adjacent reflection-spectrum envelopes is a constant. According to Fig. 1(a), the characteristics of all subgratings, such as the sampling period, the effective refractive index, and the grating segment length in the sampling period, are similar except for the Bragg period. The proposed grating structure, as shown in Fig. 1(d), can be obtained by reverse Fourier transform of the resultant reflection-spectrum envelope with broad flat-top in Fig. 1(c).

In order to determine how to obtain a flatter reflection-spectrum envelope in the DCG, we need to obtain the analytical formula of its reflection-spectrum envelope. By use of the coupling-mode theory and Fourier theory, the coupling coefficient for the conventional sampled grating can be expressed by

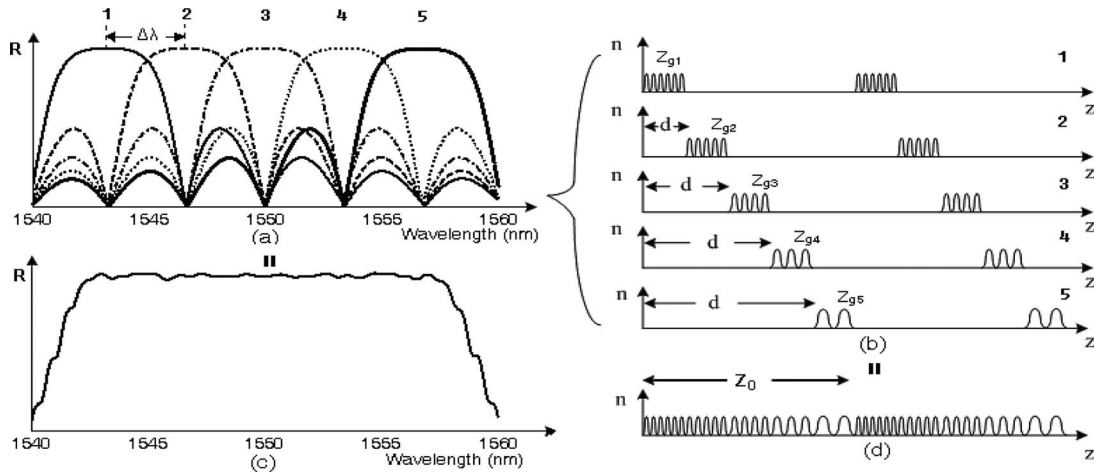


Fig. 1. DCG based on the multiple reflection-spectrum envelope concatenation technology. (a) Reflection-spectrum envelopes of conventional sampled gratings, (c) resultant reflection-spectrum envelope. (b) Structure profiles of subgratings, (d) structure profile of the DCG.

$$\kappa(n) = \kappa_0 \frac{Z_g}{Z_0} \text{sinc}(\pi n Z_g / Z_0) e^{i m n Z_g / Z_0}, \quad (1)$$

where Z_0 is the length of the sampling period and Z_g is the grating segment in the sampling period of the conventional sampled grating. The coupling coefficient of the conventional sampled grating in relation to wavelengths is [11,12]

$$\kappa(\lambda) = \kappa_0 \frac{Z_g}{Z_0} \text{sinc} \left[\pi \frac{Z_g}{Z_0} Z_0 \left(\frac{2n_{0,eff}}{\lambda} - \frac{1}{\Lambda} \right) \right] \times \exp \left[i \pi \frac{Z_g}{Z_0} \cdot Z_0 \left(\frac{2n_{0,eff}}{\lambda} - \frac{1}{\Lambda} \right) \right]. \quad (2)$$

The phase at the interface of the adjacent grating in the DCG is zero. The distance between the initial burst port of the first subgrating and the initial burst port of the other subgratings is represented by d , as shown in Fig. 1(b). The distance d introduces additional phase shift in the whole grating, so it must be considered. According to the formula of Eq. (2), the coupling coefficient of each subgrating in the DCG is defined as

$$\kappa_i(\lambda) = \kappa_0 \frac{Z_g}{Z_0} \text{sinc} \left[\pi \frac{Z_g}{Z_0} Z_0 \left(\frac{2n_{0,eff}}{\lambda} - \frac{1}{\Lambda_i} \right) \right] \exp \left[i \pi (Z_g - 2d) \left(\frac{2n_{0,eff}}{\lambda} - \frac{1}{\Lambda_i} \right) \right], \quad i = 1, 2, \dots, M, \quad (3)$$

where Λ_i is the Bragg period of the i th subgrating that must satisfy the following condition:

$$\Lambda_i = \frac{\lambda_c}{2n_{eff}} + \left[\frac{H}{Z_0} \left(\frac{\lambda_c}{2n_{eff}} \right)^2 \right], \quad (4)$$

where

$$H = m \times \left(i - \frac{M+1}{2} \right), \quad i = 1, 2, \dots, M. \quad (5)$$

M and n_{eff} are the number of subgratings and the effective refractive index of the grating waveguide, respectively; λ_c is the central wavelength of the reflection spec-

trum of the DCG; and m is an integer. The analytical formula of the resultant reflection-spectrum envelope for the digital concatenated grating is governed by

$$R_{env}(\lambda) = \tanh^2(|\kappa_1(\lambda) + \kappa_2(\lambda) + \dots + \kappa_i(\lambda) + \dots + \kappa_M(\lambda)|L). \quad (6)$$

The concatenation of reflection-spectrum envelopes can fill in the gap of the sinc spectrum envelope of the conventional sampled grating. Unlike interleaved gratings, there are no empty regions or lost reflection peaks in the DCG. Moreover, interleaving N sampled gratings makes the sampling period reduce by $1/N$ times [5], while concatenating the N sampling grating cannot change the sampling period. Unlike with phase gratings, there is no phase shift in each grating segment, including the interface of the adjacent grating segment. Furthermore, from Eqs. (4) and (5), the difference between the DCG and other modulated gratings lies in the fact that the Bragg period of each subgrating is determined only by the given length of the sampling period and the parameter m .

B. Spectrum Analysis of Digital Concatenated Gratings

The transfer matrix method is introduced to simulate the reflection spectrum of the DCG, and the reflection-spectrum envelope of the DCG is calculated by use of analytical expression of Eq. (6), which is plotted with the solid line (magenta online) outlining the peaks' profile in Fig. 2.

The parameters used for the grating simulation are $n_{0,eff} = 1.485$, $\bar{\delta}n_{eff} = 5 \times 10^{-4}$, $N = 10$, $Z_g = 0.24$ mm, and Z_0

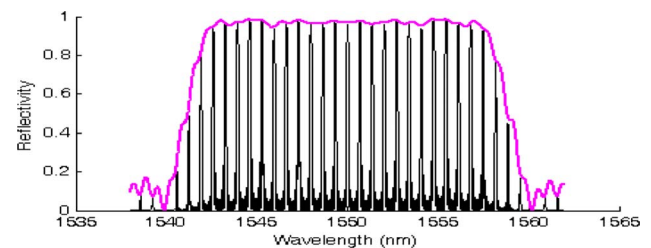


Fig. 2. (Color online) Reflection spectrum and reflection-spectrum envelope of the digital concatenated grating with five subgratings.

Table 1. Design Parameters of Each Subgrating in the DCG in Fig. 2

Order of Subgrating	Bragg Wavelength λ	Bragg Period Λ	Number of Bragg Periods	Grating Segment Length Z_g
1	1543.2292 nm	519.62 nm	462	0.24 mm
2	1546.6146 nm	520.755 nm	461	0.24 mm
3	1550 nm	521.89 nm	460	0.24 mm
4	1553.3854 nm	523.025 nm	459	0.24 mm
5	1556.7708 nm	524.16 nm	458	0.24 mm

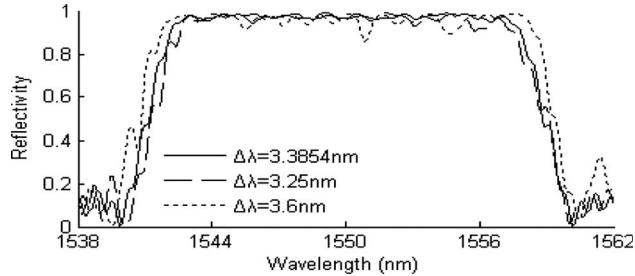


Fig. 3. Reflection-spectrum envelopes of DCGs with different spectral center separations.

$= 1.2$ mm. N is the number of sampling periods. The central wavelength λ_c is locked at 1550 nm, and the peak spacing $\delta\lambda$ of the DCG, related mainly to the central wavelength and the sampling period Z_0 , is also fixed, at 0.67708 nm. With the parameter $m=5$, the design parameter values of each subgrating listed in Table 1 conform to the formulas of Eqs. (4) and (5). The spectrum property of the DCG with five subgratings is illustrated in Fig. 2, where the spectral center separation between adjacent reflection-spectrum envelopes $\Delta\lambda$ is 3.3854 nm, which is five times the reflection peak spacing $\delta\lambda$. Up to 23 identical useful channels are obtained, as shown in Fig. 2, where the envelope of the reflection spectrum is in good agreement with the envelope calculated by the analytical expression with the magenta solid line. The accuracy of this proposed formula can be verified by the above-mentioned agreement.

To explain how the formulas of Eqs. (4) and (5) are used to optimize the grating, it is necessary to analyze the influence of the Bragg period of each subgrating on the flatness of the reflection-spectrum envelope. In Fig. 3, the reflection-spectrum envelope (solid curve) that conforms

to the design of formulas of Eqs. (4) and (5) has a smaller ripple in the envelope top than that of the other design. The fluctuation in the reflection-spectrum envelope results in some peaks in the grating being suppressed or enhanced. The more the spectral center separation deviates from the given value of 3.3854 nm, the wider the 3 dB bandwidth of the reflection-spectrum envelope is.

In Eq. (5), m is an integer, which means that the spectral center separation $\Delta\lambda$ is m times the peak spacing $\delta\lambda$, i.e., $\Delta\lambda = m * \delta\lambda$. To test the impact of the integer m , we increase m from 1 to 7 and observe the variation in the reflection spectrum of the DCG; the results obtained are demonstrated in Fig. 4. It is clear from Fig. 4 that with increase of m , the 3 dB envelope of the reflection spectrum becomes wider and the peak number of spectrum increases sharply, from 7 to 35 peaks. The three middle peaks (bottom, blue line online) in the reflection spectrum of the DCG with $m=1$ have wide linewidths. With increase of the value of m , the linewidths of the reflection peaks gradually decrease, but the number of reflection peaks increases rapidly. When $m=7$, the reflection-spectrum envelope of the DCG has a large fluctuation range. The flatness of the reflection-spectrum envelope at $m=4$, $m=5$, or $m=6$ is better than that of the gratings with other values of m . In order to obtain the flattest reflection-spectrum envelope, the grating must satisfy the conditions of Eqs. (5) and (6), with m defined as an integer $\leq M+1$ and $\geq M-1$ (M is the number of subgratings in the DCG).

3. GAUSSIAN APODIZATION ON DIGITAL CONCATENATED GRATINGS

For a clear understanding of the impact of Gaussian full apodization on the coupling strength along the grating,

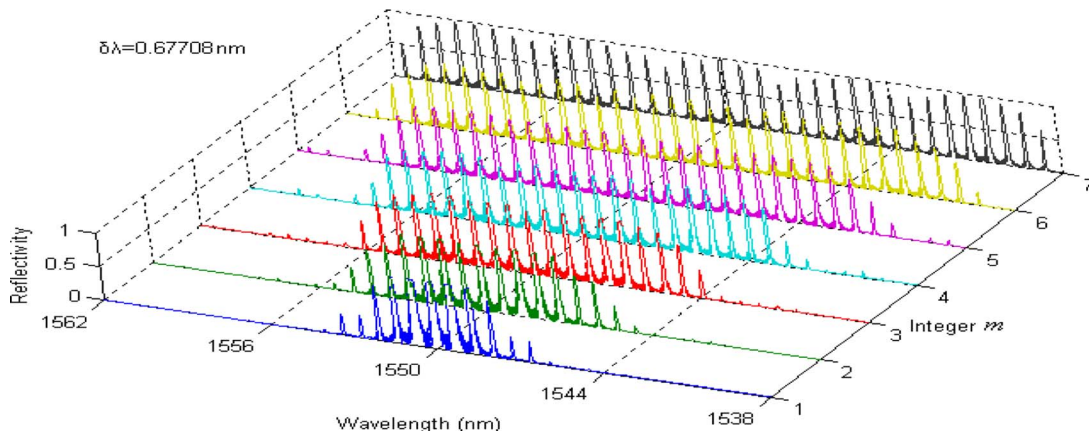


Fig. 4. (Color online) Reflection spectra of DCGs with different spectral center separations.

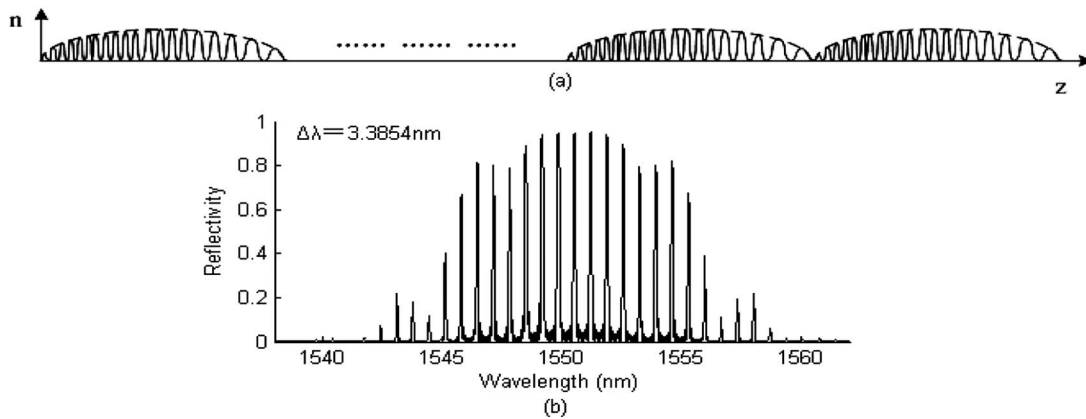


Fig. 5. DCG with Gaussian apodization on the sampling function. (a) Refractive-index profile, (b) reflection spectrum.

two types of Gaussian apodization have been introduced into the digital concatenated grating. All the designed parameters of the DCGs with Gaussian apodization are consistent with those of the DCG in Table 1. The effective refractive index of the digital grating also remains constant. One Gaussian apodization is on the sampling function, whose apodized refractive-index profile of the DCG is displayed in Fig. 5(a). This grating is called a digital concatenated Gaussian-apodized grating; its reflection spectrum is shown in Fig. 5(b). Another Gaussian apodization is on the whole grating profile function, as shown on the DCG in Fig. 6(a). This grating is called the Gaussian-apodized DCG; its reflection spectrum is shown in Fig. 6(b).

It is clear that Figs. 5 and 6 can increase our understanding of the effects of Gaussian apodization on the DCG. The Gaussian apodization on the sampling function can change the shape of the reflection-spectrum envelope in Fig. 5, where there are only 15 peaks with high reflectivity. Under the same grating parameters, the 3 dB spectrum envelope of the digital concatenated Gaussian-apodized grating is narrower than that of the DCG. Moreover, concatenating a series of Gaussian shapes cannot provide a wide and flat reflection-spectrum envelope. When compared with the DCG, the Gaussian apodization on the whole grating profile function of the DCG does not reduce the number of reflection peaks but increases the fluctuating amplitude of the reflection-spectrum envelope. The Gaussian apodization on the whole grating profile of the conventional sampled grating is similar to that of the

DCG in that both of them can eliminate the sidelobes of the reflection peaks. In other words, the Gaussian-apodized DCG is better than the digital concatenated Gaussian-apodized grating because it can offer a broad comb spectrum without sidelobes.

4. CONCLUSION

Based on the MRSEC technology, the digital concatenated grating (DCG) is proposed and designed. An analytical expression of the reflection-spectrum envelope and essential formulas on Bragg periods of the subgratings have been presented for the DCG design. The accuracy of this expression has been verified by the good agreement of the calculated reflection-spectrum envelope with the reflection peak values simulated by the transfer matrix method. The deviation from the essential formulas of Eqs. (4) and (5) would break the flatness of the reflection-spectrum envelope and lead to suppressed or enhanced reflection peaks of the gratings. In order to obtain a noticeably flat reflection-spectrum envelope, the parameter m in Eq. (6) must be an integer of $\leq M+1$ and $\geq M-1$. A large m value can increase the 3 dB bandwidth of the reflection-spectrum envelope and reduce the linewidths of the reflection peaks. Gaussian apodization on the whole profile function can not only eliminate sidelobes on each reflection peak but also provide a flatter reflection-spectrum envelope than that of the digital concatenated Gaussian-apodized grating.

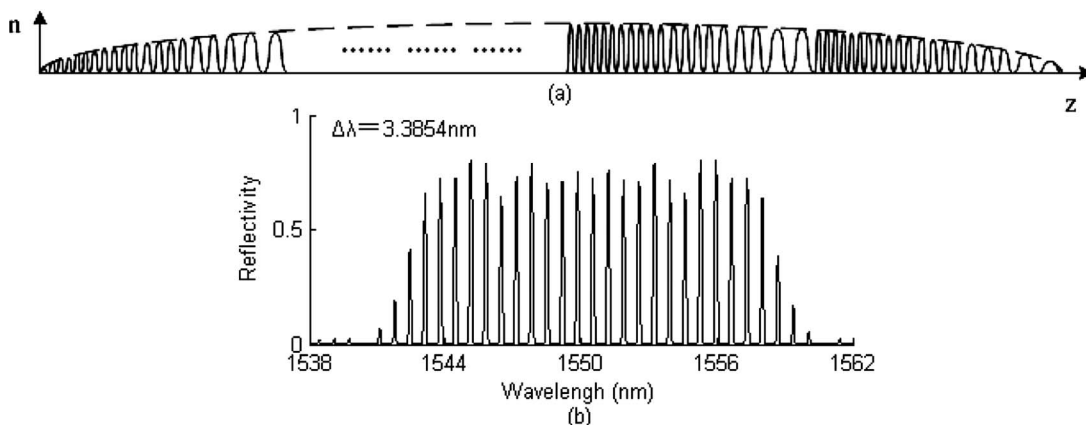


Fig. 6. DCG with Gaussian apodization on the whole grating profile. (a) Refractive-index profile, (b) reflection spectrum.

ACKNOWLEDGMENTS

The authors undertook this work with support from the National Natural Science Foundation of China under grant 60677024, the National High Technology Research Development Program of China under grant 2006AA03Z0427, and The Hong Kong Polytechnic University research grant A-PH82.

REFERENCES

1. V. Jayraman, Z.-M. Chuang, and L. A. Coldren, "Theory, design, and performance of extended tuning range semiconductor laser with sampled gratings," *IEEE J. Quantum Electron.* **29**, 1824–1834 (1993).
2. X. He, W. Li, J. Zhang, X. Huang, J. Shan, and D. Huang, "Theoretical analysis of widely tunable external cavity semiconductor laser with sampled fiber grating," *Opt. Commun.* **267**, 440–446 (2006).
3. X. F. Chen, Y. Luo, C. C. Fan, T. Wu, and S. Z. Xie, "Analytical expression of sampled Bragg gratings with chirp in the sampling period and its application in dispersion management design in a WDM system," *IEEE Photonics Technol. Lett.* **12**, 1013–1015 (2000).
4. Y. Dai, X. Chen, Y. Yao, and S. Xie, "Dispersion compensation based on sampled fiber Bragg gratings fabricated with reconstruction equivalent-chip method," *IEEE Photonics Technol. Lett.* **18**, 941–943 (2006).
5. W. H. Loh, F. Q. Zhou, and J. J. Pan, "Novel designs for sampled grating based multiplexers-demultiplexers," *Opt. Lett.* **24**, 1457–1459 (1999).
6. P. Petropoulos, M. Ibsen, M. N. Zervas, and D. J. Richardson, "Generation of a 40 GHz pulse stream by pulse multiplication with a sampled fiber Bragg grating," *Opt. Lett.* **25**, 521–523 (2000).
7. J. E. Rothenberg, R. E. Caldwell, H. Li, Y. Li, J. Popelek, Y. Sheng, Y. Wang, R. B. Wilcox, and J. Zweiback, "High-channel-count fiber Bragg gratings fabricated by phase-only sampling," in *Optical Fiber Communication Conference*, Vol. 70 of OSA Trends in Optics and Photonics (Optical Society of America, 2002), pp. 575–577.
8. H. Ishii, Y. Tohmori, Y. Yoshikuni, T. Tamamura, and Y. Kondo, "Multiple-phase-shift super structure grating DBR lasers for broad wavelength tuning," *IEEE Photonics Technol. Lett.* **5**, 613–615 (1993).
9. M. Ibsen, M. K. Durkin, M. J. Cole, and R. I. Laming, "Sinc-sampled fiber Bragg gratings for identical multiple wavelength operation," *IEEE Photonics Technol. Lett.* **10**, 842–845 (1998).
10. M. Gioannini and I. Montrosset, "Novel interleaved sampled grating mirrors for widely tunable DBR laser," *Proc. IEEE* **148**, 13–18 (2001).
11. X. He, Y. Yu, D. Huang, R. Zhang, W. Liu, and S. Jiang, "Analysis and applications of reflection-spectrum envelopes for sampled gratings," *J. Lightwave Technol.* **26**, 720–728 (2008).
12. X. He, Y. Yu, W. Liu, and D. Huang, "Analytical expression of reflection-spectrum envelope for sampled gratings," in *Proceedings of the China-Ireland International Conference on Information and Communications Technologies 2007 (CICT, 2007)*, pp. 637–645.